

Comparison of fission and quasi-fission modes

C. Simenel^{a,1}, P. McGlynn^a, A.S. Umar^b, K. Godbey^c

^aDepartment of Fundamental and Theoretical Physics and Department of Nuclear Physics and Accelerator Sciences, Research School of Physics,
The Australian National University, Canberra ACT 2601, Australia

^bDepartment of Physics and Astronomy, Vanderbilt University, Nashville, Tennessee 37235, USA

^cFacility for Rare Isotope Beams, Michigan State University, East Lansing, Michigan 48824, USA

Abstract

Quantum shell effects are known to affect the formation of fragments in nuclear fission. Shell effects also affect quasi-fission reactions occurring in heavy-ion collisions. Systematic time-dependent Hartree-Fock simulations of $^{50}\text{Ca}+^{176}\text{Yb}$ collisions show that the mass equilibration between the fragments in quasi-fission is stopped when they reach similar properties to those in the asymmetric fission mode of the ^{226}Th compound nucleus. Similar shell effects are then expected to determine the final repartition of nucleons between the nascent fragments in both mechanisms. Future experimental studies that could test these observations are discussed.

Keywords: Quasifission, fission, TDHF

1. Introduction

Nuclear fission and quasi-fission are *a priori* very different reaction mechanisms. On the one hand, fission occurs when a heavy nucleus splits into two (or more) fragments. The fissioning nucleus can be initially in its ground-state, as in spontaneous fission, or in an excited state, as in neutron-induced fission or in fission following fusion of two heavy ions. In the latter two cases, a compound nucleus is formed with equilibrated internal degrees of freedom in such a way that the fission process only depends on its excitation energy and angular momentum. On the other hand, quasi-fission is an out-of-equilibrium mechanism occurring when two heavy collision partners transfer a significant amount of nucleons through mass equilibration, before separating in fission-like fragments without the intermediate formation of a compound nucleus [1] (see [2] for a recent experimental review).

Nevertheless, both processes also exhibit some similarities. For instance, the total kinetic energy of the fragments is well approximated by the Viola systematics [3, 4], indicating a slow, damped relative motion of the fragments. In addition, the timescale for quasi-fission reactions [1, 5, 6] is of the same order as the minimum average timescale for the evolution from the compound system to the formation of the final fragments which is about 20 – 50 zs (1 zeptosecond = 1 zs = 10^{-21} s) [7]. Another similarity is that both reaction mechanisms are impacted by quantum shell effects. In fission, shell effects are able to drive the system away from mass symmetric fission, while in quasi-fission, they are expected to stop the mass equilibration process.

The purpose of this work is to compare such quasi-fission and fission modes that are driven by shell effects. Although several

shell effects are expected to occur in the compound system on its way to fission [8], our focus is on those in the nascent fragments that are responsible for the final repartition of protons and neutrons between the fragments. Neutron-induced actinide fission [9] and fission of neutron deficient actinides [10–12] reveal the presence of an asymmetric fission mode producing heavy fragments with $Z \simeq 54$ protons. Octupole (pear shape) deformed shell effects at $Z = 52$ and 56 [13] have been invoked to explain the constancy of the heavy fragment charge distribution centroid. Spherical shell effects in the ^{132}Sn region with magic numbers $Z = 50$ and $N = 82$ are also known to induce a symmetric fission mode in neutron-rich fermium isotopes [14]. In addition, other deformed shell effects are being investigated in near and sub-lead region [15–18] to explain asymmetric fission observed in this region [19, 20]. Furthermore, spherical shell effects in ^{208}Pb are predicted to induce a *super-asymmetric* mode in some superheavy nuclei (SHN) [21–27]. However, no experimental confirmation of the latter exist so far due to the difficulty of creating superheavy compound nuclei [28].

Shell effects have also been invoked to explain quasi-fission fragment mass distributions [29–38]. In particular mass equilibration is often stopped, in reactions forming SHN, when a heavy fragment in the doubly magic ^{208}Pb region is produced, even at energy well above the Coulomb barrier [34, 39, 40]. The first experimental confirmation of this effect was only recently obtained through measurement of X-rays from the quasi-fission fragments indicating an excess of fragments with the proton magic number $Z = 82$ [36]. Although this observation of a quasi-fission mode produced by shell effects could potentially be associated to the predicted super-asymmetric mode in SHN fission, there has been so far no observation (either experimentally or in numerical simulations) of quasi-fission modes that could be identified to known fission modes.

Our purpose is then to investigate quasi-fission modes in a

Email address: cedric.simenel@anu.edu.au (C. Simenel)

¹Corresponding author

heavy-ion reaction which, in the case of fusion, would produce a compound nucleus with known fission modes. We choose the $^{50}\text{Ca}+^{176}\text{Yb}$ reaction at an energy of 13% above the Coulomb barrier. The choice for this reaction is motivated by the fact that its compound nucleus, ^{226}Th , is known experimentally to have two fission modes, one symmetric and one asymmetric, both with similar yields [10–12]. Our goal is then to investigate if quasi-fission is able to populate one or both of these fission modes. Our theoretical modelling is based on the Hartree-Fock (HF) self-consistent mean-field theory with a Skyrme energy density functional (EDF), which is known to account properly for shell effects in nuclear systems [41].

2. Results

Our approach is based on three steps. First, we study the fission modes in ^{226}Th . Although theoretical modelling of fission is still an ongoing challenge [42], microscopic approaches are commonly used to investigate fission modes. Here, we construct a potential energy surface (PES) with the constrained-HF method with BCS pairing correlations. This PES is used to confirm that our choice of EDF leads to two fission modes, associated with a symmetric and an asymmetric valleys. Second, we perform a systematic study of $^{50}\text{Ca}+^{176}\text{Yb}$ collisions with the time-dependent Hartree-Fock (TDHF) theory, searching for quasi-fission trajectories. Finally, we search for potential quasi-fission modes and compare them with the fission ones. This theoretical approach is motivated by the fact that the same EDF is used to describe both nuclear structure and reaction dynamics, and by the now well established applicability of TDHF to study quasi-fission in a broad range of systems [6, 34, 39, 40, 43–48] (see [49–52] for recent reviews of TDHF applications to heavy-ion reactions). In particular, the approach has no free parameters as its only phenomenological input is the Skyrme EDF whose parameters are usually determined from properties of some nuclei and of infinite nuclear matter. We chose the SLy4d parametrisation [53] which can be used in static calculations as well as to simulate heavy-ion collisions.

To investigate the fission modes of ^{226}Th with the SLy4d Skyrme functional, a potential energy surface is constructed from mean-field solutions under constraints on the quadrupole moment

$$q_{20} = \sqrt{\frac{5}{16\pi}} \int d^3r \rho(\mathbf{r})(2z^2 - x^2 - y^2),$$

where $\rho(\mathbf{r})$ is the density of nucleons, fixing the elongation of the system, and the octupole moment

$$q_{30} = \sqrt{\frac{7}{16\pi}} \int d^3r \rho(\mathbf{r})[2z^3 - 3z(x^2 + y^2)]$$

fixing its asymmetry. For this purpose we use the SkyAx code which solves the constrained HF equations with BCS pairing correlations and axial symmetry [54]. The resulting PES in Fig. 1 confirms the existence of two fission valleys. The first valley is mass asymmetric. It is present in many actinides and

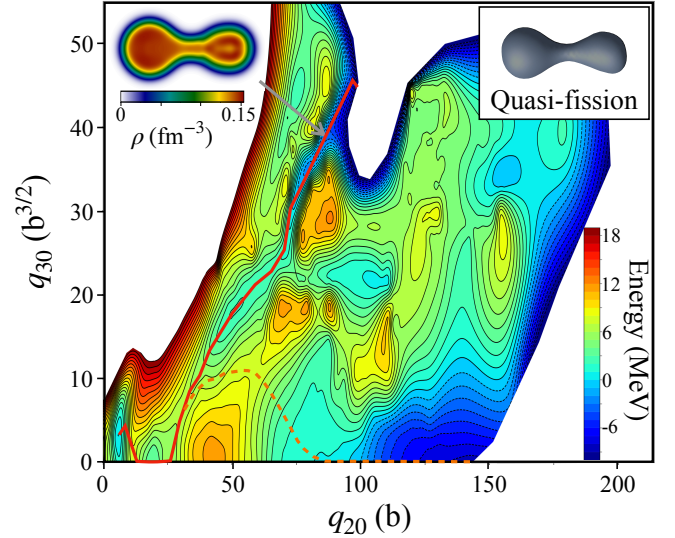


Figure 1: Potential energy surface of ^{226}Th obtained from the constrained Hartree-Fock method with BCS correlations using the SkyAx solver with quadrupole and octupole steps $\Delta q_{20} = 1.44$ b and $\Delta q_{30} = 1$ b $^{3/2}$, respectively. The red solid line shows the fission path obtained by leaving the octupole moment free. The dashed line, showing a possible path towards the symmetric valley, is to guide the eye. A density distribution for the system along the asymmetric fission path is shown for near-scission deformation indicated by the arrow. An isodensity surface (grey) at half the saturation density ($\rho_0/2 = 0.08$ fm $^{-3}$) is shown for a similar near-scission configuration (represented by star symbols in Fig. 2) obtained from a TDHF quasi-fission trajectory.

usually lead to $Z_H \approx 52 - 56$ protons in the final heavy fragments [55, 56]. This is the valley explored by the system if the octupole moment is not constrained (solid line). We also see that the system may return to symmetric shapes ($q_{30} = 0$) for little additional cost in energy (dashed line), leading to symmetric elongated fragments. Indeed, the difference in energies between the saddle point to return to the symmetric valley (overcome by the dashed line) and the first saddle point is only 1.2 MeV. We therefore expect both symmetric and asymmetric fission modes to occur with similar probabilities. These results are in good agreement with theoretical predictions using other EDF (see, e.g., [57–59]), as well as with experimental observations indicating similar yields for both modes at low excitation energy [11, 12].

Our goal is now to investigate quasi-fission modes in $^{50}\text{Ca}+^{176}\text{Yb}$ collisions which, in the case of fusion, would form the ^{226}Th compound nucleus. Quasi-fission is known to rapidly increase with the charge product Z_1Z_2 of the reactants [2]. Although experimental signatures of quasi-fission have been found in systems with Z_1Z_2 as small as 736 in the $^{16}\text{O}+^{238}\text{U}$ reaction [60], the lightest system in which quasi-fission reactions have been observed in TDHF calculations is $^{50}\text{Cr}+^{180}\text{W}$ ($Z_1Z_2 = 1776$) [44]. As TDHF predicts the most likely outcome for a given initial configuration, only a small range of orbital angular momenta L (or, equivalently, impact parameters) might lead to TDHF trajectories with quasi-fission characteristics in the $^{50}\text{Ca}+^{176}\text{Yb}$ system as it has a relatively small charge product $Z_1Z_2 = 1400$.

In this work, the TDHF3D code is used with a plane of sym-

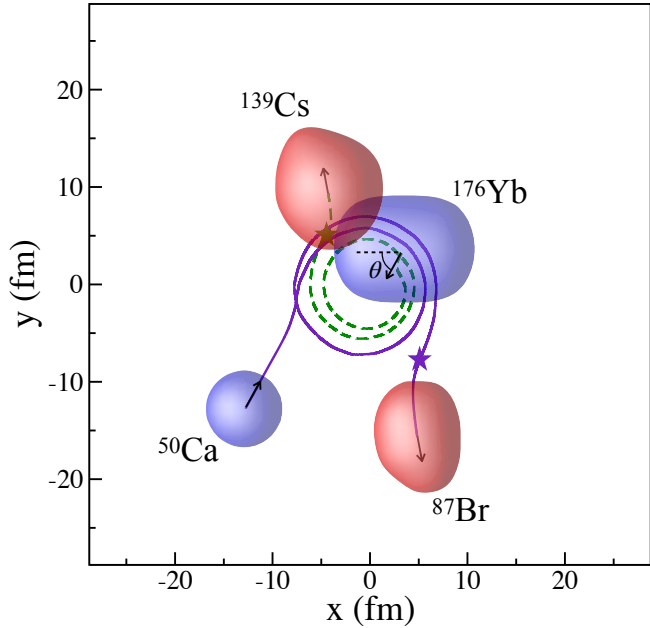


Figure 2: Example of TDHF calculation of $^{50}\text{Ca}+^{176}\text{Yb}$ with an orbital angular momentum $L = 82\hbar$ leading to quasi-fission fragments $^{87}\text{Br}+^{139}\text{Cs}$. The surfaces represent the initial (blue) and final (red) isodensities at half the saturation density $\rho_0/2 = 0.08 \text{ fm}^{-3}$. The solid and dashed lines represent the evolution of the centres of masses of the light and heavy fragments, respectively. The star symbols indicate the position on the trajectory used to represent the isodensity in Fig. 1. The x and y scales correspond to the full numerical box.

metry (the $z = 0$ reaction plane) [53]. BCS correlations are included in the initial static calculations to avoid spurious deformations in open shell nuclei. These correlations are then treated with the frozen occupation approximation in the time evolution. While the ^{50}Ca mean-field ground-state is found to be spherical, the ^{176}Yb ground-state is obtained with a prolate deformation $\beta_2 \approx 0.33$ and thus its orientation is expected to impact the reaction mechanism [61]. The centre of mass energy of the reaction is $E_{c.m.} = 172 \text{ MeV}$, corresponding to approximately 13% above the Coulomb barrier $V_B \approx 151.8 \text{ MeV}$ according to the systematics of Swiatecki *et al.* [62]. This energy is large enough to ensure that all initial orientations of the prolate deformed ^{176}Yb may lead to contact between the collision partners and then potentially contribute to quasi-fission [60]. The initial distance between the centres of mass of the collision partners is 22.6 fm. As the angle of emission of the fragments is unknown prior to a calculation, large Cartesian grids of $72 \times 72 \times (28/2) \times \Delta x^3$ with a mesh size $\Delta x = 0.8 \text{ fm}$ are used to allow for a full description of the exit channel with well separated final fragments. We performed 40 TDHF calculations with four initial orientations of ^{176}Yb deformation axis (forming an angle of 0, 45, 90, and 135 degrees with respect to the axis joining the initial centres of mass), and with a $\Delta L = 2\hbar$ step in orbital angular momentum, for a total of 14,000 CPU hours on Intel Xeon Scalable ‘Cascade Lake’ processors. The results are compiled in Supplemental Material Table 1.

An example of resulting quasi-fission trajectory is shown in Fig. 2 for an orbital angular momentum $L = 82\hbar$ and an ori-

entation of $\theta \approx 62.0$ degrees between the ^{176}Yb initial velocity vector and its deformation axis. The position of the fragments is obtained at each time by computing the centres of mass of the density distributions on each side of the neck. The resulting trajectories are represented by the solid and dashed lines in Fig. 2. We see that the system undergoes more than a full rotation, during which about 37 nucleons (in average) are transferred from the heavy fragment to the light one. The total contact time, defined as the time during which the neck density exceeds half saturation density $\rho_0/2 \approx 0.08 \text{ fm}^{-3}$, is $\tau \approx 22.9 \text{ zs}$ for this collision. This contact time and the large amount of mass transfer between reactants are typical of quasi-fission reactions [1, 5].

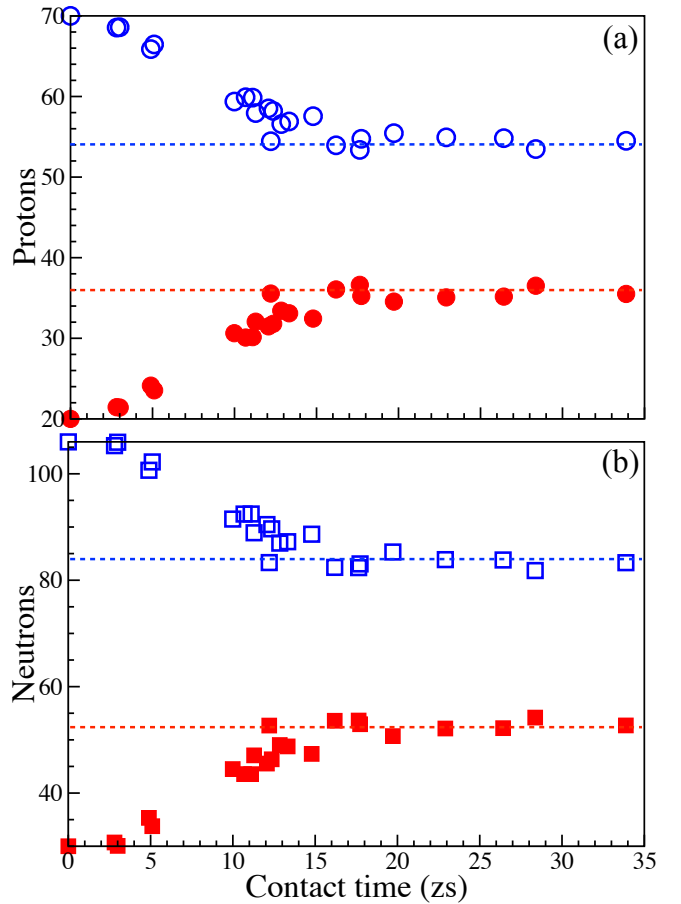


Figure 3: (a) Proton (circles) and (b) neutron (squares) numbers in the heavy (open symbols) and light (filled symbols) fragments as a function of contact time. The dashed lines represent possible asymptotic values at $Z_H \approx 54$, $Z_L \approx 36$, $N_H \approx 84$, and $N_L \approx 52$.

Quasi-fission trajectories were searched for up to approximately 30 zs contact times. Although a slow quasi-fission component with longer contact times is observed experimentally [2], this upper limit is of the order of the longest quasi-fission times observed in TDHF calculations [6]. We therefore consider that the system has fused when the contact time reaches $\tau \sim 31 \text{ zs}$ (unless an increase of elongation indicates a likely quasi-fission at a later time, in which case the calculations is run up to $\tau \sim 35 \text{ zs}$), which occurs essentially below critical angular momentum L_c that depends on the orientation of the

target. Collisions that lead to contact with the side of ^{176}Yb are found to have smaller critical value $L_c \sim 60\hbar$, while collisions with its tip lead to $L_c \sim 80\hbar$. At large L , only few nucleons are exchanged in quasi-elastic collisions, occurring at $L_q \sim 68\hbar$ ($\sim 96\hbar$) in collisions with the side (tip) of ^{176}Yb . For a given orientation, quasi-fission is obtained for $L_c \lesssim L \lesssim L_q$. (Note that in few cases we observe quasi-fission for $L < L_c$, see Supplemental Material Tab. 1.)

The number of protons and neutrons in the outgoing fragments are plotted in Fig. 3 as a function of the contact time. A correlation is observed at short contact times ($\tau \lesssim 13$ zs) where nucleons are transferred from the heavy to the light fragment. At longer contact times, however, this correlation is lost, with constant numbers of protons and neutrons $Z_L \approx 36$, $N_L \approx 52$, $Z_H \approx 54$ and $N_H \approx 84$ in the light and heavy fragments, respectively, indicating a stop of the mass equilibration process. Interestingly, this occurs when the fragments have reached the same numbers of neutrons and protons as the asymmetric fission fragments of ^{226}Th , which is a first indication that these fission and quasi-fission modes are similar.

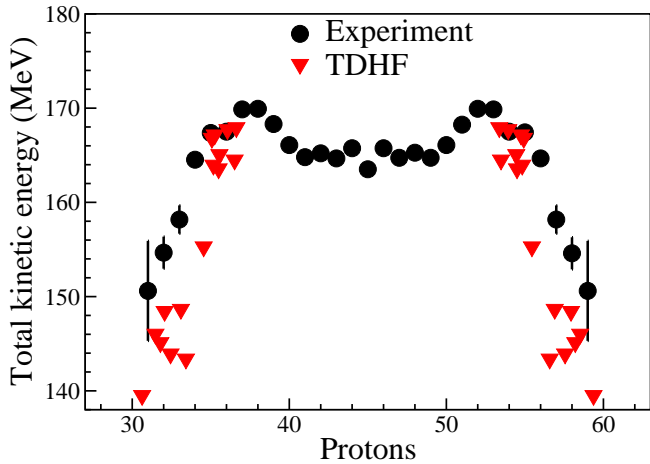


Figure 4: Experimental average TKE of ^{226}Th fission fragments (circles) from Ref. [11] and TDHF predictions of quasi-fission fragments TKE (triangles).

As most of the shell effects fixing the final asymmetry in nascent fission fragments are deformed shell effects, it is important to compare the shape of fragments as well as the number of protons and neutrons. Experimentally, the shape of the system at scission is inferred indirectly through the total kinetic energy (TKE) of the fragments. Indeed, for a similar mass and charge partition, higher TKE are larger for more compact fragments, while elongated fragments lead to lower TKE. Figure 4 provides a comparison between experimental TKE of fission fragments and TKE of quasi-fission fragments obtained from TDHF by summing kinetic and Coulomb energy between the fragments (see, e.g., [63]). We see that, for the fragments which have reached the $Z_L/Z_H \approx 36/54$ partition, the TKE are similar in both processes, indicating similar shapes of the systems at scission. However, for more asymmetric splits, quasi-fission leads to smaller TKE than fission which could be attributed to differences in the dynamics. Indeed, larger asymmetries in quasi-fission are obtained for the most peripheral colli-

sions (larger L) inducing shapes which can significantly differ to those in fission. The fact that quasi-fission fragments with $Z_L/Z_H \approx 36/54$ partition have a similar shape than those produced in the asymmetric fission mode of ^{226}Th is further supported by a comparison of the densities near scission in Fig. 1.

The observation that the mass equilibration is stopped when the fragments have reached proton and neutron numbers, as well as shapes, that are similar to those in the asymmetric fission mode, is an indication that both modes should have the same origin in terms of shell effects. In particular, the octupole deformed shell effects at $Z_H \approx 52 - 56$, that were invoked as a mechanism allowing the heavy fragment to acquire pear shapes for a small cost (if any) in energy [13], could also be responsible for stopping the mass equilibration process in quasi-fission.

3. Conclusions

Like fission, quasifission is affected by shell effects through valleys in the potential energy surfaces [64, 65]. Here, we have shown that quasifission may populate the asymmetric fission mode of ^{226}Th . However, the symmetric fission mode, which has similar yields as the asymmetric one in ^{226}Th , is not observed in our TDHF simulations of quasi-fission. A possible explanation is that the shell effects responsible for the asymmetric fission mode are strong enough to stop mass equilibration in every quasi-fission trajectory. Alternatively, longer contact times may be needed for quasi-fission trajectories leading to symmetric fragments. In that case, beyond mean-field fluctuations and correlations that build up over time may be required. It would be interesting to investigate this system with the stochastic mean-field approach which, in addition to incorporating such fluctuations as demonstrated in the case of fission [66], might allow the system to explore paths with smaller probabilities thanks to these fluctuations (whereas in TDHF, only the most likely mean-field drives the dynamics).

Experimentally, quasi-fission properties are often investigated by comparing reactions forming similar compound nuclei from different entrance channels [67–69]. A simultaneous investigation of quasi-fission and fission modes in the same system could be achieved by comparing $^{48,50}\text{Ca} + ^{176}\text{Yb}$ (beams of ^{50}Ca with sufficient intensity should be available at FRIB [70]) in which one expects both quasi-fission and fusion-fission reactions, with $^{16,18}\text{O} + ^{208}\text{Pb}$ (forming the same compound nuclei) in which quasi-fission is expected to be negligible.

An experimental confirmation of strong similarities between (at least some) fission and quasi-fission modes could help finding indications of the existence of theoretically predicted fission modes in nuclei that are experimentally difficult to produce, such as in superheavy nuclei. Naturally, quasi-fission could not entirely replace the experimental investigations of fission fragment distributions for the following reasons: (i) There is no guarantee that a mode observed in quasi-fission would also be present in the fission of the compound nucleus; (ii) The relative abundance of competing quasi-fission modes could be very different to that of fission modes; (iii) Not all fission modes are expected to be necessarily produced in quasi-fission.

Acknowledgments

We thank D. J. Hinde for his continuous support to this work, as well as R. Bernard for his help with the construction of the PES and a careful reading of the manuscript. Useful discussions with K. J. Cook and M. Dasgupta are also acknowledged. This work has been supported by the Australian Research Council Discovery Project (project number DP190100256) funding schemes, by the U.S. Department of Energy under grant Nos. DE-SC0013847 (Vanderbilt University) and DE-SC0013365 (Michigan State University), and by the NNSA Cooperative Agreement DE-NA0003885. This work was also supported by computational resources provided by the Australian Government through the National Computational Infrastructure (NCI) under the ANU Merit Allocation Scheme.

References

- [1] J. Töke, R. Bock, G. X. Dai, A. Gobbi, S. Gralla, K. D. Hildenbrand, J. Kuzminski, W. F. J. Müller, A. Olmi, H. Stelzer, B. B. Back, S. Bjørnholm, Quasi-fission: The mass-drift mode in heavy-ion reactions, *Nucl. Phys. A* 440 (1985) 327–365. doi:10.1016/0375-9474(85)90344-6.
- [2] D. J. Hinde, M. Dasgupta, E. C. Simpson, Experimental studies of the competition between fusion and quasifission in the formation of heavy and superheavy nuclei, *Prog. Part. Nucl. Phys.* 118 (2021) 103856. doi:10.1016/j.ppnp.2021.103856.
- [3] V. E. Viola, K. Kwiatkowski, M. Walker, Systematics of fission fragment total kinetic-energy release, *Phys. Rev. C* 31 (1985) 1550–1552. doi:10.1103/PhysRevC.31.1550.
- [4] D. J. Hinde, J. R. Leigh, J. J. M. Bokhorst, J. O. Newton, R. L. Walsh, J. W. Boldeman, Mass-split dependence of the pre- and post-scission neutron multiplicities for fission of ^{251}Es , *Nucl. Phys. A* 472 (1987) 318–332. doi:10.1016/0375-9474(87)90213-2.
- [5] R. du Rietz, E. Williams, D. J. Hinde, M. Dasgupta, M. Evers, C. J. Lin, D. H. Luong, C. Simenel, A. Wakhle, Mapping quasifission characteristics and timescales in heavy element formation reactions, *Phys. Rev. C* 88 (2013) 054618. doi:10.1103/PhysRevC.88.054618.
- [6] C. Simenel, K. Godbey, A. S. Umar, Timescales of Quantum Equilibration, Dissipation and Fluctuation in Nuclear Collisions, *Phys. Rev. Lett.* 124 (2020) 212504. doi:10.1103/PhysRevLett.124.212504.
- [7] D. J. Hinde, D. Hilscher, H. Rossner, B. Gebauer, M. Lehmann, M. Wilpert, Neutron emission as a probe of fusion-fission and quasi-fission dynamics, *Phys. Rev. C* 45 (1992) 1229–1259. doi:10.1103/PhysRevC.45.1229.
- [8] R. Bernard, C. Simenel, G. Blanchon, Quantum shell effects on the path to fission of atomic nuclei, Submitted.
- [9] D. A. Brown, M. B. Chadwick, R. Capote, A. C. Kahler, A. Trkov, M. W. Herman, A. A. Sonzogni, Y. Danon, A. D. Carlson, M. Dunn, D. L. Smith, G. M. Hale, G. Arbanas, R. Arcilla, C. R. Bates, B. Beck, B. Becker, F. Brown, R. J. Casperson, J. Conlin, D. E. Cullen, M.-A. Descalle, R. Firestone, T. Gaines, K. H. Guber, A. I. Hawari, J. Holmes, T. D. Johnson, T. Kawano, B. C. Kiedrowski, A. J. Koning, S. Kopecky, L. Leal, J. P. Lestone, C. Lubitz, J. I. M. Damián, C. M. Mattoon, E. A. McCutchan, S. Mughabghab, P. Navratil, D. Neudecker, G. P. A. Nobre, G. Noguere, M. Paris, M. T. Pigni, A. J. Plompen, B. Pritychenko, V. G. Pronyaev, D. Roubtsov, D. Rochman, P. Romano, P. Schillebeeckx, S. Simakov, M. Sin, I. Sirakov, B. Sleaford, V. Sobes, E. S. Soukhovitskii, I. Stetcu, P. Talou, I. Thompson, S. van der Marck, L. Welsch-Sherrill, D. Wiarda, M. White, J. L. Wormald, R. Q. Wright, M. Zerkle, G. Žerovnik, Y. Zhu, ENDF/B-VIII.0: The 8th Major Release of the Nuclear Reaction Data Library with CIELO-project Cross Sections, New Standards and Thermal Scattering Data, *Nucl. Dat. Sheets* 148 (2018) 1–142, special Issue on Nuclear Reaction Data. doi:10.1016/j.nds.2018.02.001.
- [10] K.-H. Schmidt, S. Steinhäuser, C. Böckstiegel, A. Grewe, A. Heinz, A. R. Junghans, J. Benlliure, H.-G. Clerc, M. de Jong, J. Müller, M. Pfützner, B. Voss, Relativistic radioactive beams: A new access to nuclear-fission studies, *Nucl. Phys. A* 665 (2000) 221–267. doi:10.1016/S0375-9474(99)00384-X.
- [11] C. Böckstiegel, S. Steinhäuser, K.-H. Schmidt, H.-G. Clerc, A. Grewe, A. Heinz, M. de Jong, A. R. Junghans, J. Müller, B. Voss, Nuclear-fission studies with relativistic secondary beams: Analysis of fission channels, *Nucl. Phys. A* 802 (2008) 12–25. doi:10.1016/j.nuclphysa.2008.01.012.
- [12] A. Chatillon, J. Taïeb, H. Alvarez-Pol, L. Audouin, Y. Ayyad, G. Bélier, J. Benlliure, G. Boutoux, M. Caamaño, E. Casarejos, D. Cortina-Gil, A. Ebran, F. Farget, B. Fernández-Domínguez, T. Gorbina, L. Grente, A. Heinz, H. T. Johansson, B. Jurado, A. Kelić Heil, N. Kurz, B. Laurent, J.-F. Martin, C. Nociforo, C. Paradela, E. Pellereau, S. Pietri, A. Prochazka, J. L. Rodríguez-Sánchez, H. Simon, L. Tassan-Got, J. Vargas, B. Voss, H. Weick, Experimental study of nuclear fission along the thorium isotopic chain: From asymmetric to symmetric fission, *Phys. Rev. C* 99 (2019) 054628. doi:10.1103/PhysRevC.99.054628.
- [13] G. Scamps, C. Simenel, Impact of pear-shaped fission fragments on mass-asymmetric fission in actinides, *Nature* 564 (2018) 382–385. doi:10.1038/s41586-018-0780-0.
- [14] E. K. Hulet, J. F. Wild, R. J. Dougan, R. W. Lougheed, J. H. Landrum, A. D. Dougan, M. Schadel, R. L. Hahn, P. A. Baisden, C. M. Henderson, R. J. Dupzyk, K. Sümmerer, G. R. Bethune, Biomodal symmetrical fission observed in the heaviest elements, *Phys. Rev. Lett.* 56 (1986) 313–316. doi:10.1103/PhysRevLett.56.313.
- [15] G. Scamps, C. Simenel, Effect of shell structure on the fission of sub-lead nuclei, *Phys. Rev. C* 100 (2019) 041602(R). doi:10.1103/PhysRevC.100.041602.
- [16] K. Mahata, C. Schmitt, Shilpi Gupta, A. Shrivastava, G. Scamps, K.-H. Schmidt, Evidence for the general dominance of proton shells in low-energy fission, arXiv:2007.16184. URL <https://arxiv.org/abs/2007.16184>
- [17] E. Prasad, D. J. Hinde, M. Dasgupta, D. Y. Jeung, A. C. Berriman, B. M. A. Swinton-Bland, C. Simenel, E. C. Simpson, R. Bernard, E. Williams, K. J. Cook, D. C. Rafferty, C. Sengupta, J. F. Smith, K. Vo-Phuoc, J. Walshe, Systematics of the mass-asymmetric fission of excited nuclei from ^{176}Os to ^{206}Pb , *Phys. Lett. B* 811 (2020) 135941. doi:10.1016/j.physletb.2020.135941.
- [18] B. M. A. Swinton-Bland, M. A. Stoyer, A. C. Berriman, D. J. Hinde, C. Simenel, J. Buete, T. Tanaka, K. Banerjee, L. T. Bezzina, I. P. Carter, K. J. Cook, M. Dasgupta, D. Y. Jeung, C. Sengupta, E. C. Simpson, K. Vo-Phuoc, Mass-asymmetric fission of $^{205,207,209}\text{Bi}$ at energies close to the fission barrier using proton bombardment of $^{204,206,208}\text{Pb}$, *Phys. Rev. C* 102 (2020) 054611. doi:10.1103/PhysRevC.102.054611.
- [19] A. N. Andreyev, J. Elseviere, M. Huyse, P. Van Duppen, S. Antalic, A. Barzakh, N. Bree, T. E. Cocolios, V. F. Comas, J. Diriken, D. Fedorov, V. Fedosseev, S. Franchoo, J. A. Heredia, O. Ivanov, U. Köster, B. A. Marsh, K. Nishio, R. D. Page, N. Patronis, M. Seliverstov, I. Tsekhanovich, P. Van den Bergh, J. Van De Walle, M. Venhart, S. Vermote, M. Veselsky, C. Wagemans, T. Ichikawa, A. Iwamoto, P. Möller, A. J. Sierk, New Type of Asymmetric Fission in Proton-Rich Nuclei, *Phys. Rev. Lett.* 105 (2010) 252502. doi:10.1103/PhysRevLett.105.252502.
- [20] E. Prasad, D. J. Hinde, K. Ramachandran, E. Williams, M. Dasgupta, I. P. Carter, K. J. Cook, D. Y. Jeung, D. H. Luong, S. McNeil, C. S. Palshetkar, D. C. Rafferty, C. Simenel, A. Wakhle, J. Khuyagbaatar, Ch. E. Düllmann, B. Lommel, B. Kindler, Observation of mass-asymmetric fission of mercury nuclei in heavy ion fusion, *Phys. Rev. C* 91 (2015) 064605. doi:10.1103/PhysRevC.91.064605.
- [21] D. N. Poenaru, R. A. Gherghescu, W. Greiner, Heavy-Particle Radioactivity of Superheavy Nuclei, *Phys. Rev. Lett.* 107 (2011) 062503. doi:10.1103/PhysRevLett.107.062503.
- [22] M. Warda, A. Zdeb, L. M. Robledo, Cluster radioactivity in superheavy nuclei, *Phys. Rev. C* 98 (2018) 041602. doi:10.1103/PhysRevC.98.041602.
- [23] Z. Matheson, S. A. Giuliani, W. Nazarewicz, J. Sadhukhan, N. Schunck, Cluster radioactivity of $^{294}_{118}\text{Og}_{176}$, *Phys. Rev. C* 99 (2019) 041304. doi:10.1103/PhysRevC.99.041304.
- [24] D. N. Poenaru, R. A. Gherghescu, α decay and cluster radioactivity of nuclei of interest to the synthesis of $Z = 119, 120$ isotopes, *Phys. Rev. C* 97 (2018) 044621. doi:10.1103/PhysRevC.97.044621.
- [25] Y. L. Zhang, Y. Z. Wang, Systematic study of cluster radioactivity of

- superheavy nuclei, *Phys. Rev. C* 97 (2018) 014318. doi:10.1103/PhysRevC.97.014318.
- [26] K. P. Santhosh, C. Nithya, Systematic studies of α and heavy-cluster emissions from superheavy nuclei, *Phys. Rev. C* 97 (2018) 064616. doi:10.1103/PhysRevC.97.064616.
- [27] C. Ishizuka, X. Zhang, M. D. Usang, F. A. Ivanyuk, S. Chiba, Effect of the doubly magic shell closures in ^{132}Sn and ^{208}Pb on the mass distributions of fission fragments of superheavy nuclei, *Phys. Rev. C* 101 (2020) 011601. doi:10.1103/PhysRevC.101.011601.
- [28] E. Vardaci, M. G. Itkis, I. M. Itkis, G. Knyazheva, E. M. Kozulin, Fission and quasifission toward the superheavy mass region, *J. Phys. G: Nucl. Part. Phys.* 46 (2019) 103002. doi:10.1088/1361-6471/ab3118.
- [29] M. G. Itkis, J. Äystö, S. Beghini, A. A. Bogachev, L. Corradi, O. Dorvaux, A. Gadea, G. Giardina, F. Hanappe, I. M. Itkis, M. Jandel, J. Kliman, S. V. Khlebnikov, G. N. Kniyazeva, N. A. Kondratiev, E. M. Kozulin, L. Krupa, A. Latina, T. Materna, G. Montagnoli, Yu. Ts. Oganessian, I. V. Pokrovsky, E. V. Prokhorova, N. Rowley, V. A. Rubchenya, A. Ya. Rusanov, R. N. Sagaidak, F. Scarlassara, A. M. Stefanini, L. Stuttge, S. Szilner, M. Trotta, W. H. Trzaska, D. N. Vakhin, A. M. Vinodkumar, V. M. Voskressenski, V. I. Zagrebaev, Shell effects in fission and quasi-fission of heavy and superheavy nuclei, *Nucl. Phys. A* 734 (2004) 136–147. doi:10.1016/j.nuclphysa.2004.01.022.
- [30] K. Nishio, H. Ikezoe, S. Mitsuoka, I. Nishinaka, Y. Nagame, Y. Watanabe, T. Ohtsuki, K. Hirose, S. Hofmann, Effects of nuclear orientation on the mass distribution of fission fragments in the reaction of $^{36}\text{S} + ^{238}\text{U}$, *Phys. Rev. C* 77 (2008) 064607. doi:10.1103/PhysRevC.77.064607.
- [31] E. M. Kozulin, G. N. Knyazheva, I. M. Itkis, M. G. Itkis, A. A. Bogachev, L. Krupa, T. A. Loktev, S. V. Smirnov, V. I. Zagrebaev, J. Äystö, W. H. Trzaska, V. A. Rubchenya, E. Vardaci, A. M. Stefanini, M. Cinausero, L. Corradi, E. Fioretto, P. Mason, G. F. Prete, R. Silvestri, S. Beghini, G. Montagnoli, F. Scarlassara, F. Hanappe, S. V. Khlebnikov, J. Kliman, A. Brondi, A. Nitto, R. Moro, N. Gelli, S. Szilner, Investigation of the reaction $^{64}\text{Ni} + ^{238}\text{U}$ being an option of synthesizing element 120, *Phys. Lett. B* 686 (2010) 227–232. doi:10.1016/j.physletb.2010.02.041.
- [32] K. Nishio, S. Mitsuoka, I. Nishinaka, H. Makii, Y. Wakabayashi, H. Ikezoe, K. Hirose, T. Ohtsuki, Y. Aritomo, S. Hofmann, Fusion probabilities in the reactions $^{40,48}\text{Ca} + ^{238}\text{U}$ at energies around the Coulomb barrier, *Phys. Rev. C* 86 (2012) 034608. doi:10.1103/PhysRevC.86.034608.
- [33] E. M. Kozulin, G. N. Knyazheva, S. N. Dmitriev, I. M. Itkis, M. G. Itkis, T. A. Loktev, K. V. Novikov, A. N. Baranov, W. H. Trzaska, E. Vardaci, S. Heinz, O. Beliuskina, S. V. Khlebnikov, Shell effects in damped collisions of ^{88}Sr with ^{176}Yb at the Coulomb barrier energy, *Phys. Rev. C* 89 (2014) 014614. doi:10.1103/PhysRevC.89.014614.
- [34] A. Wakhle, C. Simenel, D. J. Hinde, M. Dasgupta, M. Evers, D. H. Luong, R. du Rietz, E. Williams, Interplay between Quantum Shells and Orientation in Quasifission, *Phys. Rev. Lett.* 113 (2014) 182502. doi:10.1103/PhysRevLett.113.182502.
- [35] M. G. Itkis, E. Vardaci, I. M. Itkis, G. N. Knyazheva, E. M. Kozulin, Fusion and fission of heavy and superheavy nuclei (experiment), *Nucl. Phys. A* 944 (2015) 204–237. doi:10.1016/j.nuclphysa.2015.09.007.
- [36] M. Morjean, D. J. Hinde, C. Simenel, D. Y. Jeung, M. Airiau, K. J. Cook, M. Dasgupta, A. Drouart, D. Jacquet, S. Kalkal, C. S. Palshetkar, E. Prasad, D. Rafferty, E. C. Simpson, L. Tassan-Got, K. Vo-Phuoc, E. Williams, Evidence for the Role of Proton Shell Closure in Quasifission Reactions from X-Ray Fluorescence of Mass-Identified Fragments, *Phys. Rev. Lett.* 119 (2017) 222502. doi:10.1103/PhysRevLett.119.222502.
- [37] D. J. Hinde, D. Y. Jeung, E. Prasad, A. Wakhle, M. Dasgupta, M. Evers, D. H. Luong, R. du Rietz, C. Simenel, E. C. Simpson, E. Williams, Sub-barrier quasifission in heavy element formation reactions with deformed actinide target nuclei, *Phys. Rev. C* 97 (2018) 024616. doi:10.1103/PhysRevC.97.024616.
- [38] E. M. Kozulin, E. Vardaci, W. H. Trzaska, A. A. Bogachev, I. M. Itkis, A. V. Karpov, G. N. Knyazheva, K. V. Novikov, Evidence of quasifission in the ^{180}Hg composite system formed in the $^{68}\text{Zn} + ^{112}\text{Sn}$ reaction, *Phys. Lett. B* 819 (2021) 136442. doi:10.1016/j.physletb.2021.136442.
- [39] V. E. Oberacker, A. S. Umar, C. Simenel, Dissipative dynamics in quasifission, *Phys. Rev. C* 90 (2014) 054605. doi:10.1103/PhysRevC.90.054605.
- [40] A. S. Umar, V. E. Oberacker, C. Simenel, Fusion and quasifission dynamics in the reactions $^{48}\text{Ca} + ^{249}\text{Bk}$ and $^{50}\text{Ti} + ^{249}\text{Bk}$ using a time-dependent Hartree-Fock approach, *Phys. Rev. C* 94 (2016) 024605. doi:10.1103/PhysRevC.94.024605.
- [41] M. Bender, P.-H. Heenen, P.-G. Reinhard, Self-consistent mean-field models for nuclear structure, *Rev. Mod. Phys.* 75 (2003) 121–180. doi:10.1103/RevModPhys.75.121.
- [42] M. Bender, R. Bernard, G. Bertsch, S. Chiba, J. J. Dobaczewski, N. Dubray, S. Giuliani, K. Hagino, D. Lacroix, Z. Li, P. Magierski, J. Maruhn, W. Nazarewicz, J. Pei, S. Péru-Desenfants, N. Pillet, J. Randrup, D. Regnier, P.-G. Reinhard, L. M. Robledo, W. Ryssens, J. Sadhukhan, G. Scamps, N. Schunck, C. Simenel, J. Skalski, I. Stetcu, P. Stevenson, A. S. Umar, M. Verriere, D. Vretenar, M. Warda, S. Åberg, Future of Nuclear Fission Theory, *J. Phys. G: Nucl. Part. Phys.* 47 (2020) 113002. doi:10.1088/1361-6471/abab4f.
- [43] A. S. Umar, V. E. Oberacker, C. Simenel, Shape evolution and collective dynamics of quasifission in the time-dependent Hartree-Fock approach, *Phys. Rev. C* 92 (2015) 024621. doi:10.1103/PhysRevC.92.024621.
- [44] K. Hammerton, Z. Kohley, D. J. Hinde, M. Dasgupta, A. Wakhle, E. Williams, V. E. Oberacker, A. S. Umar, I. P. Carter, K. J. Cook, J. Greene, D. Y. Jeung, D. H. Luong, S. D. McNeil, C. S. Palshetkar, D. C. Rafferty, C. Simenel, K. Stiefel, Reduced quasifission competition in fusion reactions forming neutron-rich heavy elements, *Phys. Rev. C* 91 (2015) 041602(R). doi:10.1103/PhysRevC.91.041602.
- [45] K. Sekizawa, K. Yabana, Time-dependent Hartree-Fock calculations for multinucleon transfer and quasifission processes in the $^{64}\text{Ni} + ^{238}\text{U}$ reaction, *Phys. Rev. C* 93 (2016) 054616. doi:10.1103/PhysRevC.93.054616.
- [46] L. Guo, C. Shen, C. Yu, Z. Wu, Isotopic trends of quasifission and fusion-fission in the reactions $^{48}\text{Ca} + ^{239,244}\text{Pu}$, *Phys. Rev. C* 98 (2018) 064609. doi:10.1103/PhysRevC.98.064609.
- [47] H. Zheng, S. Burrello, M. Colonna, D. Lacroix, G. Scamps, Connecting the nuclear equation of state to the interplay between fusion and quasifission processes in low-energy nuclear reactions, *Phys. Rev. C* 98 (2018) 024622. doi:10.1103/PhysRevC.98.024622.
- [48] K. Godbey, A. S. Umar, C. Simenel, Deformed shell effects in $^{48}\text{Ca} + ^{249}\text{Bk}$ quasifission fragments, *Phys. Rev. C* 100 (2019) 024610. doi:10.1103/PhysRevC.100.024610.
- [49] C. Simenel, Nuclear quantum many-body dynamics, *Eur. Phys. J. A* 48 (2012) 152. doi:10.1140/epja/i2012-12152-0.
- [50] C. Simenel, A. S. Umar, Heavy-ion collisions and fission dynamics with the time-dependent Hartree-Fock theory and its extensions, *Prog. Part. Nucl. Phys.* 103 (2018) 19–66. doi:10.1016/j.pnpnp.2018.07.002.
- [51] Kazuyuki Sekizawa, TDHF Theory and Its Extensions for the Multinucleon Transfer Reaction: A Mini Review, *Front. Phys.* 7 (2019) 20. doi:10.3389/fphy.2019.00020.
- [52] P. D. Stevenson, M. C. Barton, Low-energy heavy-ion reactions and the Skyrme effective interaction, *Prog. Part. Nucl. Phys.* 104 (2019) 142–164. doi:10.1016/j.pnpnp.2018.09.002.
- [53] Ka-Hae Kim, Takaharu Otsuka, Paul Bonche, Three-dimensional TDHF calculations for reactions of unstable nuclei, *J. Phys. G: Nucl. Part. Phys.* 23 (1997) 1267. doi:10.1088/0954-3889/23/10/014.
- [54] P.-G. Reinhard, B. Schuetrumpf, J. A. Maruhn, The Axial Hartree-Fock + BCS Code SkyAx, *Comput. Phys. Commun.* 258 (2021) 107603. doi:10.1016/j.cpc.2020.107603.
- [55] A. N. Andreyev, K. Nishio, K.-H. Schmidt, Nuclear fission: a review of experimental advances and phenomenology, *Rep. Prog. Phys.* 81 (2017) 016301. doi:10.1088/1361-6633/aa82eb.
- [56] Karl-Heinz Schmidt, Beatriz Jurado, Review on the progress in nuclear fission—experimental methods and theoretical descriptions, *Rep. Prog. Phys.* 81 (2018) 106301. doi:10.1088/1361-6633/aacfa7.
- [57] N. Dubray, H. Goutte, J.-P. Delaroche, Structure properties of ^{226}Th and $^{256,258,260}\text{Fm}$ fission fragments: Mean-field analysis with the Gogny force, *Phys. Rev. C* 77 (2008) 014310. doi:10.1103/PhysRevC.77.014310.
- [58] H. Tao, J. Zhao, Z. P. Li, T. Nikšić, D. Vretenar, Microscopic study of induced fission dynamics of ^{226}Th with covariant energy density functionals, *Phys. Rev. C* 96 (2017) 024319. doi:10.1103/PhysRevC.96.024319.
- [59] R. N. Bernard, N. Pillet, L. M. Robledo, M. Anguiano, Description of the

- asymmetric to symmetric fission transition in the neutron-deficient thorium isotopes: Role of the tensor force, *Phys. Rev. C* 101 (2020) 044615. doi:10.1103/PhysRevC.101.044615.
- [60] D. J. Hinde, M. Dasgupta, J. R. Leigh, J. C. Mein, C. R. Morton, J. O. Newton, H. Timmers, Conclusive evidence for the influence of nuclear orientation on quasifission, *Phys. Rev. C* 53 (1996) 1290–1300. doi:10.1103/PhysRevC.53.1290.
- [61] K. Godbey, C. Simenel, A. S. Umar, Microscopic predictions for the production of neutron-rich nuclei in the reaction $^{176}\text{Yb} + ^{176}\text{Yb}$, *Phys. Rev. C* 101 (2020) 034602. doi:10.1103/PhysRevC.101.034602.
- [62] W. J. Świątecki, K. Siwek-Wilczyńska, J. Wilczyński, Fusion by diffusion. II. Synthesis of transfermium elements in cold fusion reactions, *Phys. Rev. C* 71 (2005) 014602. doi:10.1103/PhysRevC.71.014602.
- [63] C. Simenel, A. S. Umar, Formation and dynamics of fission fragments, *Phys. Rev. C* 89 (2014) 031601(R). doi:10.1103/PhysRevC.89.031601.
- [64] V. Zagrebaev, W. Greiner, Unified consideration of deep inelastic, quasifission and fusion-fission phenomena, *J. Phys. G: Nucl. Part. Phys.* 31 (2005) 825. doi:10.1088/0954-3899/31/7/024.
- [65] Valery Zagrebaev, Walter Greiner, Shell effects in damped collisions: A new way to superheavies, *J. Phys. G: Nucl. Part. Phys.* 34 (2007) 2265. doi:10.1088/0954-3899/34/11/004.
- [66] Y. Tanimura, D. Lacroix, S. Ayik, Microscopic Phase-Space Exploration Modeling of ^{258}Fm Spontaneous Fission, *Phys. Rev. Lett.* 118 (2017) 152501. doi:10.1103/PhysRevLett.118.152501.
- [67] A. Yu. Chizhov, M. G. Itkis, I. M. Itkis, G. N. Kniajeva, E. M. Kozulin, N. A. Kondratiev, I. V. Pokrovsky, R. N. Sagaidak, V. M. Voskressensky, A. V. Yerein, L. Corradi, A. Gadea, A. Latina, A. M. Stefanini, S. Szilner, M. Trotta, A. M. Vinodkumar, S. Beghini, G. Montagnoli, F. Scarlassara, A. Y. Rusanov, F. Hanappe, O. Dorvaux, N. Rowley, L. Stuttgé, Unexpected entrance-channel effect in the fission of $^{216}\text{Ra}^*$, *Phys. Rev. C* 67 (2003) 011603. doi:10.1103/PhysRevC.67.011603.
- [68] R. Rafei, R. G. Thomas, D. J. Hinde, M. Dasgupta, C. R. Morton, L. R. Gasques, M. L. Brown, M. D. Rodriguez, Strong evidence for quasifission in asymmetric reactions forming ^{202}Po , *Phys. Rev. C* 77 (2008) 024606. doi:10.1103/PhysRevC.77.024606.
- [69] E. Williams, D. J. Hinde, M. Dasgupta, R. du Rietz, I. P. Carter, M. Evers, D. H. Luong, S. D. McNeil, D. C. Rafferty, K. Ramachandran, A. Wakhle, Evolution of signatures of quasifission in reactions forming curium, *Phys. Rev. C* 88 (2013) 034611. doi:10.1103/PhysRevC.88.034611.
- [70] Thomas Glasmacher, Bradley Sherrill, Witek Nazarewicz, Alexandra Gade, Paul Mantica, Jie Wei, Georg Bollen, Brad Bull, Facility for Rare Isotope Beams Update for *Nuclear Physics News*, *Nucl. Phys. News* 27 (2017) 28–33. doi:10.1080/10619127.2017.1317176.

Appendix. SUPPLEMENTAL MATERIAL

Table 1: TDHF calculations for $^{50}\text{Ca} + ^{176}\text{Yb}$ collisions at $E_{c.m.} = 172$ MeV. The ^{176}Yb deformation axis has an angle of 0, 45, 90 or 135 degrees with the line connecting the centre of masses of the nuclei in the TDHF initial condition. θ is the angle between the ^{176}Yb velocity vector in the initial TDHF condition and its deformation axis. L is the initial orbital angular momentum of the collision. The contact time τ is given in zeptoseconds ($1 \text{ zs} = 10^{-21} \text{ s}$). The calculations are stopped when the contact time exceeds $\tau \sim 31 \text{ zs}$ (unless the system is on its way to split in two fragments, in which case the calculation is run up to $\tau \sim 35 \text{ zs}$). The number of protons and neutrons in the heavy and light fragments are obtained from integration of the proton and neutron densities in the outgoing fragments. The total kinetic energy (TKE) is the sum of the kinetic energy of the fragments and of their Coulomb potential energy assuming point like fragments in the last TDHF iteration.

θ (deg.)	L (\hbar)	τ (zs)	Z_H	N_H	Z_L	N_L	TKE (MeV)
14.7	70	>31.39					
15.1	72	>31.39					
15.5	74	>31.39					
16.0	76	>31.39					
16.4	78	28.37	53.48	81.82	36.52	54.18	164.50
16.8	80	>31.39					
17.3	82	12.07	58.52	90.46	31.48	45.54	146.02
17.7	84	10.68	59.91	92.43	30.09	43.57	129.50
18.1	86	11.11	59.86	92.45	30.14	43.55	131.91
18.6	88	5.10	66.46	102.23	23.54	33.77	132.02
59.5	70	>31.22					
59.9	72	>31.22					
60.3	74	33.88	54.50	83.29	35.50	52.71	163.56
60.7	76	26.42	54.83	83.80	35.17	52.20	163.95
61.1	78	>31.23					
61.6	80	>31.23					
62.0	82	22.91	54.93	83.87	35.07	52.13	166.80
62.4	84	16.19	53.94	82.41	36.06	53.59	167.72
62.8	86	17.64	53.37	82.37	36.63	53.63	167.93
63.3	88	17.73	54.75	83.06	35.25	52.94	167.16
63.7	90	12.21	54.45	83.31	35.55	52.69	165.07
64.1	92	11.29	57.94	88.92	32.06	47.08	148.43
64.6	94	9.99	59.37	91.49	30.63	44.51	139.51
65.0	96	3.00	68.59	105.93	21.41	30.07	137.42
100.5	50	>30.96					
100.9	52	>30.96					
101.3	54	>30.96					
101.7	56	>30.96					
102.1	58	>30.96					
102.6	60	>30.96					
103.0	62	13.33	56.90	87.23	33.10	48.77	148.65
103.4	64	14.79	57.56	88.64	32.44	47.36	143.92
103.8	66	12.85	56.58	86.97	33.42	49.03	143.38
104.3	68	12.36	58.21	89.65	31.79	46.35	145.12
104.7	70	4.90	65.88	100.66	24.12	35.34	132.51
147.4	60	>31.17					
147.8	62	>31.17					
148.2	64	>31.17					
148.6	66	19.72	55.45	85.30	34.55	50.70	155.28
149.0	68	2.81	68.55	105.29	21.45	30.71	135.83